# The effect of LaNiO3 bottom electrode thickness on ferroelectric and dielectric properties of (100) oriented PbZr0.53Ti0.47O3 films

G.S. Wang, Denis Remiens, Caroline Soyer, El Hadj Dogheche, Eric Cattan

# The effect of $LaNiO_3$ bottom electrode thickness on ferroelectric and dielectric properties of (1 0 0) oriented $PbZr_{0.53}Ti_{0.47}O_3$ films

G.S. Wang[a,b,*], D. Rémiens[a], C. Soyer[a], E. Dogheche[a], E. Cattan[a]

[a] *IEMN– DOAE– MIMM team, CNRS UMR 8520, Bat. P3, Cité scientifique, Villeneuve d'Ascq 59655, France*
[b] *National Laboratory for Infrared Physics, Shanghai Institute of Technical Physics, Chinese cademy of Sciences, Yutian Road 500, Shanghai 200083, PR China*

The (1 0 0) oriented $LaNiO_3$ (LNO) films with different thickness were prepared on $SiO_2$/Si substrate by a modified metallorganic decomposition process. $PbZr_{0.53}Ti_{0.47}O_3$ (PZT) films (~1 μm) subsequently deposited on LNO by modified sol–gel process. The X-ray diffraction measurements show PZT films exhibit a single perovskite phase with (1 0 0) preferred orientation. $\alpha_{100} > 94\%$ can be obtained for PZT deposited on LNO bottom electrode with thickness greater than 60 nm. SEM measurements show the PZT films have a columnar structure. The LNO thickness effect on $P_r$, $E_c$, and dielectric constant were investigated and showed that the thickness of the LNO bottom electrode caused drastic changes in $P_r$, dielectric constant and dielectric loss. Sub-switching fields dependence of permittivity were investigated for PZT films and showed that both reverible and irreversible component of the permittivity increase with the thickness of LNO electrode.

*Keywords:* A1. X-ray diffraction; B1. Perovskite; B2. Ferroelectric materials

## 1. Introduction

The coexistence of tetragonal and rhombohedral phases in pseudo-perovskite $PbZr_{0.53}Ti_{0.47}O_3$ (PZT) with a composition near the morphotropic phase boundary (MPB) enhances the dielectric and

*Corresponding author. IEMN–DOAE–MIMM team, CNRS UMR 8520, Bat. P3, Cité scientifique, Villeneuve d'Ascq 59655, France. Tel.: +33 03 20 43 40 18; fax: 33 03 27 51 14 39.
*E-mail address:* Genshui.Wang@univ-lille1.fr (G.S. Wang).

piezoelectric properties. The recent efforts have therefore been made to integrate this PZT material onto MEMS devices, such as ultrasonic micromotors, linear actuators, micropumps, and transducers for ultrasound imaging [1,2]. The properties of PZT films for MEMS application are greatly different from those of bulk ceramics due to fine grains, extrinsic stress, and substrate effects. The properties of PZT films depend on many parameters, including preferred orientation, composition, microstructure, films thickness, buffer layer and dopants [2,3]. In view of the orientation of PZT films, the largest piezoelectric coefficient and dielectric constant were found in (1 0 0) oriented films [4–6]. It was demonstrated experimentally and theoretically that the (1 0 0)-oriented PZT films were more suitable for the MEMS sensors and actuating applications [6–8]. It is well known that the films orientation is influenced by processing parameters such as properties of precursor solution, pyrolysis temperature, annealing temperature, heating rate, seeding layers, and bottom electrode.

Fabrication of electrode for ferroelectric film capacitor is important in device applications. In the past few years, the $LaNiO_3$ (LNO) was verified as an electrode for application in ferroelectric film capacitor. LNO is a perovskite-type metallic oxide with a lattice parameter of 3.84 Å, which matches well with ferroelectric films such as PZT and BST [9,10]. Therefore, the conducting textured LNO film is a favorable candidate for electrode of ferroelectric thin films. There are many references reported preparation and electric properties of PZT thin films ($<500$ nm) on LNO coated Si substrate [9,11–15]. Few work on preparation and properties of (1 0 0) PZT thick films (0.5–10 μm, which is more suitable for MEMS application) on LNO electrode. Among all the methods of preparing PZT thick films, a wet chemical process is widely employed due to its easy and low cost preparation, chemical homogeneity and facility of stoichiometry control [3,12]. This study was conducted to investigate the properties of highly (1 0 0) oriented $PbZr_{0.53}Ti_{0.47}O_3$ thick ($\sim$1 μm) films on $LaNiO_3$ coated silicon for MEMS application by chemical solution routes.

## 2. Experimental procedure

For PZT films, the starting materials were tri-hydrated lead acetate, $Pb(CH_3COO)_2 \cdot 3H_2O$ (Aldrich Co., purity 99 + %), zirconium(IV) *n*-propoxide, $Zr(OCH_2CH_2CH_3)_4$ (Aldrich Co., 70 wt% solution in 1-propanol), and titanium isopropoxide, $Ti(OCH(CH_3)_2)_4$ (Aldrich Co., purity 97%), 2-methoxyethanl, $CH_3OCH_2CH_2OH$ (Aldrich Co., purity 99.3 + %) were used as solvent. Appropriate amount of acetylacetone $CH_3OCH_2COCH_3$ (Aldrich Co., purity 99 + %) is added to solution to stable the solution. And appropriate amount of polyethylene glycol (PEG) (with molecular weight of 200 and PZT/PEG ratio of 0.02 mol/1 ml) was added to solution to avoid the crack in annealing process. The precursor solutions were prepared with Zr/Ti ratio of $\frac{53}{47}$. 15% mole excess lead was added to solution to compensate for lead oxide loss in annealing process and suppress the pyrochlore formation. The concentration of the final solution is 0.6 M. For $LaNiO_3$ (LNO) films, the starting materials were lanthanum acetate, $La(CH_3COO)3 \cdot .xH_2O$ (Aldrich Co., purity 99.9%) and nickel acetate, $Ni(CH_3COO)_2 \cdot 4H_2O$ (Aldrich Co., purity 98%). Acetate acid, $CH_3COOH$ (Aldrich Co., purity 99.7 + %) and deion water (with $CH_3COOH/H_2O$ ratio of 5:1) were used as solvent. The concentration of final solution is 0.2 M.

A rapid thermal annealing process (JIPELEC-FAV4 system) realized the crystallization of the LNO and PZT thin films. The LNO films were prepared by spinning the precursor solution on $SiO_2$/Si substrate at 3000 rpm for 30 s. Each annealing layer was dried at 180 °C for 180 s, then prefired at 360 °C for 180 s, following annealed at 700 °C for 180 s. Consequently, the PZT thin films were deposited by spinning the solution on LNO coated Si substrates at 3000 rpm for 30 s. Each layer of the films was dried at 200 °C for 180 s, then prefired at 400 °C for 300 s to remove the residual organics, following annealed at 650 °C for 300 s. The average thickness of a single-annealed layer for LNO and PZT were measured about 30 and 95 nm, respectively. The desired films with thickness of LNO and PZT were achieved by repeated spin-coating and heating treatment cycles. The

whole heating treatment was conducted in pure oxygen atmosphere. Samples A, B, C, D, E, F represent PZT on LNO coated $SiO_2$/Si substrate with different LNO thickness of 30, 60, 90, 120, 150, and 180 nm, respectively.

The structure of PZT films is analyzed by X-ray diffraction (XRD) using a Ni filtered Cu-$\kappa$ $\alpha$ radiation source (D5000, SIEMENS). The microstructure and the thickness of the films are examined using scanning electron microscopy. In order to preparing the capacitor cells for electric test, Pt top electrodes were prepared by a sputtering instrument through a photolithography process. Ferroelectric properties of the capacitor were measured by TF2000A ferroelectric test system using a low-voltage mode ($<25$ V) and high-voltage mode. The dielectric properties were measured by HP4192A multi-frequency LCR meter.

## 3. Results and discussions

Fig. 1(a) shows the XRD patterns of LNO films on $SiO_2$/Si substrate with different thickness. It can be seen that LNO films shows (1 0 0) preferred orientation, and the intensity of (2 0 0) peak increase with thickness from 30 to 150 nm. Above 150 nm, the intensity of (2 0 0) peak shows a little decrease. The sheet resistance for LNO with different thickness are shown by inset figure in Fig. 1(a), as thickness bigger than 120 nm, the sheet resistance is smaller than 200Ω/□. Fig. 1(b) shows the XRD patterns of PZT on LNO coated $SiO_2$/Si substrate with different LNO thickness. A, B, C, D, E, F represent thickness of 30, 60, 90, 120, 150, and 180 nm, respectively. It can be seen that PZT films exhibit a single perovskite phase with (1 0 0) preferred orientation. The (1 0 0)-orientation parameter, $\alpha_{100}$, was calculated from the relative intensity of the (1 0 0), (1 1 0), and (1 1 1) diffraction peaks, i.e.,

$$\alpha_{100} = I_{100}/(I_{100} + I_{110} + I_{111}). \quad (1)$$

The $\alpha_{100}$ for all the samples were calculated and listed in Table 1. $\alpha_{100} > 94\%$ can be obtained for PZT deposited on LNO bottom electrode with thickness bigger than 60 nm. The results indicate

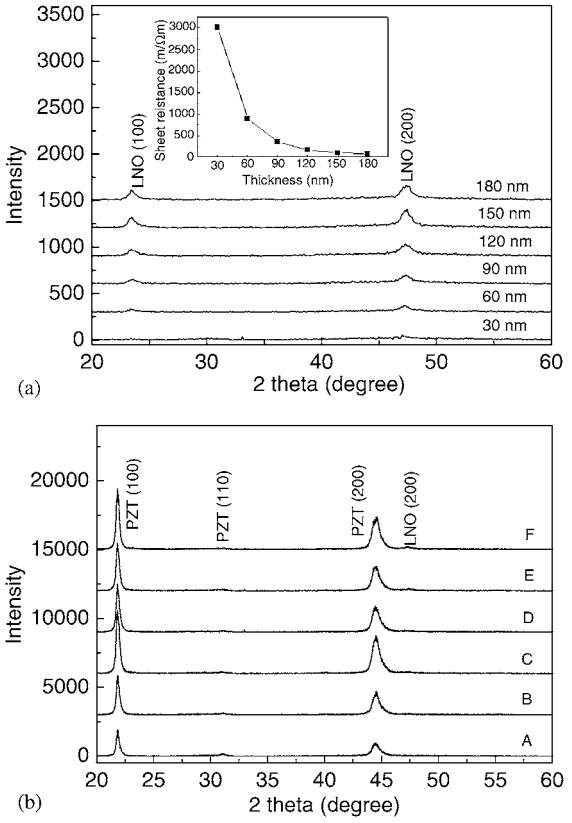


Fig. 1. XRD patterns of PZT and LNO films: (a) LNO films on $SiO_2$/Si substrate with different thickness. A, B, C, D, E, F represent thickness of 30, 60, 90, 120, 150, and 180 nm, respectively. Inset figure shows the sheet resistance of LNO with different thickness. (b) PZT on LNO coated $SiO_2$/Si substrate with different LNO thickness. A, B, C, D, E, F represent thickness of 30, 60, 90, 120, 150, and 180 nm, respectively.

Table 1
(1 0 0) orientaion parameter, $P_r$, $E_c$ of PZT on LNO coated $SiO_2$/Si substrate with different LNO thickness.

| Sample | $\alpha_{100}$ (%) | $P_r$ (μC/cm$^2$) | $E_c$ (kV/cm) |
|---|---|---|---|
| A | 87.2 | — | — |
| B | 94.1 | 8 | 40 |
| C | 96.3 | 10.7 | 39 |
| D | 95.5 | 12.5 | 38 |
| E | 95.7 | 12.5 | 37 |
| F | 96.6 | 12.3 | 34 |

A, B, C, D, E, F represent thickness of 30, 60, 90, 120, 150, and 180 nm, respectively.

that the crystallization and growth of the PZT thin films are significantly influenced by the (1 0 0)-oriented LNO films due to well matching of crystallographic and chemical structure between the LNO and PZT [9,11,12]. High $\alpha_{100}$ value maybe due to heterogeneous nucleation is dominant nucleation process for PZT grown on LNO [16].

Fig. 2 shows the XRD patterns of PZT on LNO coated $SiO_2$/Si substrate with different LNO thickness in the range of 43–46° with a more precise $2\theta$ scanning. It can be seen that the peak becomes more wide as increases the thickness of LNO. When the peaks were fitted by two peaks of (0 0 2) and (2 0 0), it can be seen that the peak of the (0 0 2) move to smaller angle, and the peak of (2 0 0) is stable as the thickness of LNO increases.

Some cracks can be observed in sample A (LNO thickness is 30 nm). As thickness of LNO bigger than 60 nm, there is not any crack can be observed, and PZT thick films have a uniform, pinhole-free, and mirrorlike surface. Fig. 3 shows the SEM image of the cross-section of the PZT films fabricated on LNO (180 nm)/$SiO_2$/Si substrate. It can be seen that PZT films have a columnar structure. There is a critical thickness for cracking of PZT films on silicon-based substrate [17] due to the thermal mismatch in the coefficient of thermal expansion between PZT and Si substrat. Use LNO buffer layer can release tensile stress between PZT and Si substrate. Thicker LNO electrode is necessary to deposit crack-free thicker PZT films on Si substrate.

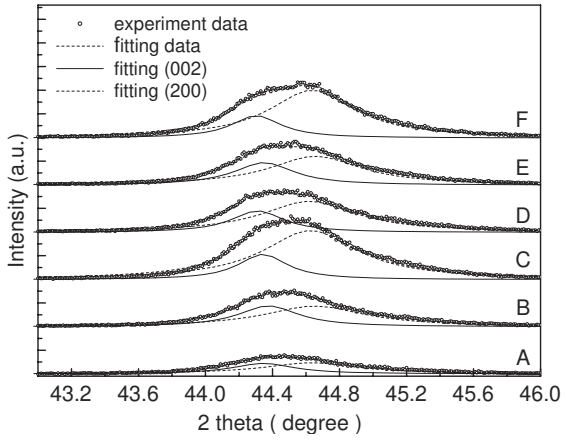


Fig. 2. XRD patterns of PZT on LNO coated $SiO_2$/Si substrate with different LNO thickness in the range of 43–46° with a more precise $2\theta$ scanning.

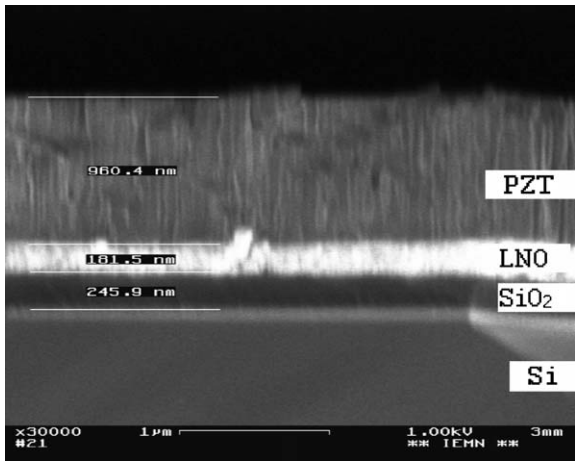


Fig. 3. SEM image of the cross-section of the PZT films fabricated on LNO (180 nm)/$SiO_2$/Si substrate.

Fig. 4(a) shows $P$– $V$ hysteresis loops of PZT on LNO(90 nm)/$SiO_2$/Si with different applied voltage, the hysteresis loops are saturated as the applied voltage beyond 40 V. Fig. 4(b) shows $P$– $V$ hysteresis loops of PZT on LNO coated $SiO_2$/Si substrate with different LNO thickness, B, C, D, E, F represent thickness of 60, 90, 120, 150, and 180 nm, respectively. $P_r$, $E_c$ of PZT on LNO coated $SiO_2$/Si substrate with different LNO thickness list in Table 1. $E_c$ shows a little decrease as increase the thickness of LNO, and $P_r$ is saturated as LNO thickness beyond 120 nm. All the samples show smaller $E_c$ than thin films in reference [12,13] due to the thickness of PZT in present work is bigger than in reference. And (1 0 0) oriented PZT show small $P_r$ due to [1 0 0] direction is not the possible polarization orientation in both tetragonal, for which that is [0 0 1] direction, and rhombohedral phases, for which that is [1 1 1] direction. In present samples, the [0 0 1] direction are the smaller portion compare with [1 0 0] direction (see Fig. 2).

Fig. 5 shows dielectric constant as a function of frequency for Pt/PZT/LNO capacitors with different LNO thickness. B, C, D, E, F represent thickness of 60, 90, 120, 150, and 180 nm, respectively. The dielectric constant shows an increase trend with increase the thickness of

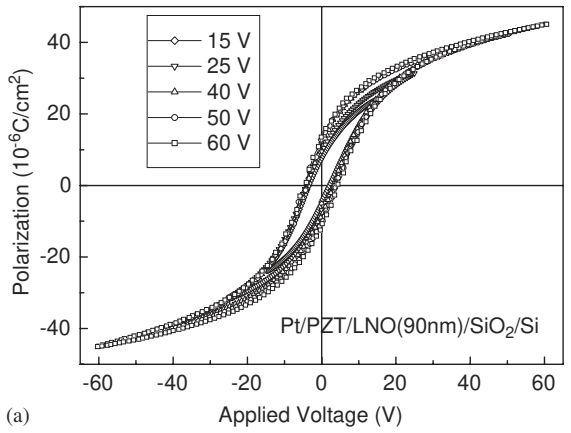


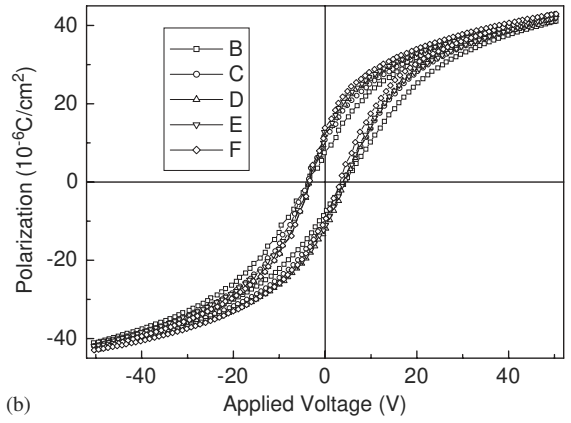


Fig. 4. Polarization hysteresis loops of PZT films: (a) $P$–$V$ hysteresis loops of PZT on LNO(90 nm)/$SiO_2$/Si with different applied voltage; (b) $P$–$V$ hysteresis loops of PZT on LNO coated $SiO_2$/Si substrate with different LNO thickness. B, C, D, E, F represent thickness of 60, 90, 120, 150, and 180 nm, respectively.

LNO. The dielectric loss with different thickness of LNO at 10 kHz are list in Table 2. Dielectric loss decrease rapidly as thickness of LNO from 60 to 120 nm, and little change with thickness from 120 nm to 180 nm. The dielectric properties of PZT are enhanced as the thickness of LNO increase may be explained that the change of the resistance of bottom electrode. (see the inset figure of Fig. 1)

The permittivity of PZT films on LNO with different thickness were measured as a function of AC driving electric field. In this work the maximum applied AC field was 1.3 MV/m, which is smaller than half of the coercive field for this

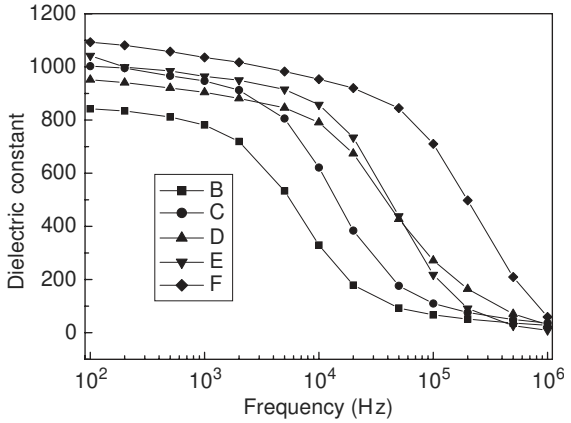


Fig. 5. Dielectric constant as a function of frequency for Pt/PZT/LNO capacitors with with different LNO thickness. B, C, D, E, F represent thickness of 60, 90, 120, 150, and 180 nm, respectively.

Table 2
Dielectric properties of PZT on LNO coated $SiO_2$/Si substrate with different LNO thickness.

| Sample | tan δ | $\varepsilon_{init}$ (nF/m) | $\alpha(10^{-16}$F/V) |
|---|---|---|---|
| B | 0.217 | 2.6754 | −0.567 |
| C | 0.103 | 4.5828 | 0.866 |
| D | 0.058 | 6.8374 | 3.932 |
| E | 0.053 | 7.4453 | 5.723 |
| F | 0.051 | 7.8658 | 7.908 |

B, C, D, E, F represent thickness of 60, 90, 120, 150, and 180 nm, respectively.

PZT films. This field region will be referred as sub-switching field. In this sub-switching field region, permittivity can be described by Rayleigh law [18]

$$\varepsilon_{33} = \varepsilon_{init} + \alpha E_0, \quad (2)$$

where $\varepsilon_{33}$ is total permittivity of PZT films, $\varepsilon_{init}$ is due to intrinsic lattice and reversible domain wall contributions to the permittivity, and $\alpha E_0$ is due to irreversible displacement of walls. Fig. 6 shows field dependence of permittivity for Pt/PZT/LNO capacitors with different LNO thickness. B, C, D, E, F represent thickness of 60, 90, 120, 150, and 180 nm, respectively. The measurement frequency is 10 kHz. The full lines represent best fits to Eq. (2) and fitting parameters are shown in Table 2. Both reverible and irreversible component of the

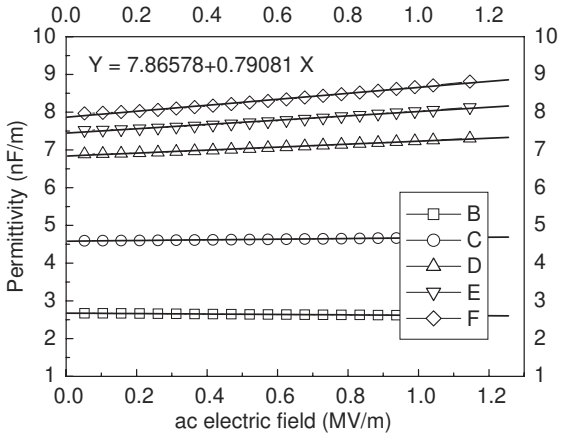


Fig. 6. Field dependence of permittivity for for Pt/PZT/LNO capacitors with with different LNO thickness. B, C, D, E, F represent thickness of 60, 90, 120, 150, and 180 nm, respectively. The full lines represent best fits to Eq. (2) and fitting parameters are shown in Table 2.

permittivity increase with the thickness of LNO electrode. As thickness of LNO is 150 nm, the $\varepsilon_{init}$ and $\alpha$ for PZT (0.96 μm) are 7.4453 nF/m and $5.723 \times 10^{-16}$F/V, respectively, which can compare 1.3 μm PZT on Pt [18]. The biggest $\varepsilon_{init}$ and $\alpha$ are obtained for PZT films on 180 nm LNO electrode. This maybe due to thicker LNO is easy to release the stress between PZT and Si substrate.

## 4. Conclusion

The highly (1 0 0) oriented ($\alpha_{100} > 0.94$) $PbZr_{0.53}Ti_{0.47}O_3$ thick films have been successfully deposited on LNO coated silicon substrate by modified sol–gel process. The effect of LNO thickness on properties of PZT were investigated. The thickness of the LNO bottom electrode caused drastic changes in $P_r$, dielectric constant, dielectric loss and sub-switching field behavior. Control the thickness can obtain the ideal properties for special application. This highly (1 0 0) oriented PZT thick films on LNO coated silicon substrate are potential for MEMS applications.

## Acknowledgements

This work was supported by the post-doctoral project provide by France ministry of research and new technology.

## References

[1] D. Rémiens, Piezoelectric materials for macro/micro system, Research Signpost, Kerala India, 2003.
[2] T. Haccart, E. Cattan, D. Rémiens, S. Hiboux, P. Muralt, Appl. Phys. Lett. 76 (2000) 3292.
[3] W. Gong, J.F. Li, X. Chu, Z. Gui, L. Li, J. Appl. Phys. 96 (2004) 590.
[4] L. Lian, N.R. Sottos, J. Appl. Phys. 87 (2000) 3941.
[5] W. Gong, J.F. Li, X. Chu, Z. Gui, L. Li, Acta Materialia 52 (2004) 2787.
[6] X.H. Du, J. Zheng, U. Belegundu, K. Uchino, Appl. Phys. Lett. 72 (1998) 2421.
[7] D.V. Taylor, D. Damjanovic, Appl. Phys. Lett. 76 (2000) 1615.
[8] J. Ouyang, S.Y. Yang, L. Chen, R. Ramesh, A.L. Roytburd, Appl. Phys. Lett. 85 (2004) 278.
[9] X.J. Meng, J.G. Cheng, J.L. Sun, H.J. Ye, S.L. Guo, J.H. Chu, J. Crystal Growth 220 (2000) 100.
[10] G.S. Wang, J.G. Cheng, X.J. Meng, J. Yu, Z.Q. Lai, J. Tang, S.L. Guo, J.H. Chu, Appl. Phys. Lett. 78 (2001) 4172.
[11] S.H. Hu, G.J. Hu, X.J. Meng, G.S. Wang, J.L. Sun, J.H. Chu, N. Dai, J. Crystal Growth 260 (2004) 109.
[12] S.H. Hu, X.J. Meng, G.S. Wang, J.L. Sun, D.X. Li, J. Crystal Growth 264 (2004) 307.
[13] Li. Jiankang, Yao. Xi, Mater. Lett. 58 (2004) 3447.
[14] B.G. Chae, Y.S. Yang, S.H. Lee, M.S. Jang, S.J. Lee, S.H. Kim, W.S. Baek, S.C. Kwon, Thin Solid Films 410 (2002) 107.
[15] C.H. Lin, P.A. Friddle, C.H. Ma, A. Daga, H. Chen, J. Appl. Phys. 90 (2001) 1509.
[16] R.W. Schwartz, J.A. Voigt, B.A. Tuttle, D.A. Payne, T.L. Reichert, R.S. Dasalla, J. Mater. Res. 12 (1997) 444.
[17] M.-H. Zhao, R. Fu, D. Lu, T.–Y. Zhang, Acta Materialia 50 (2002) 4241.
[18] D.V. Taylor, D. Damjanovic, J. Appl. Phys. 82 (1997) 1973.